

Panton-Valentine Leucocidin of *Staphylococcus aureus* Induces Oxidative Stress and Neurotransmitter Imbalance in a Retinal Explant Model

Mathieu Wurtz,^{1,2} Elisa Ruhland,³ XuanLi Liu,¹ Izzie-Jacques Namer,³ Viola Mazzoleni,¹ Dan Lipsker,⁴ Daniel Keller,¹ Gilles Prévost,¹ and David Gaucher^{1,2}

¹University of Strasbourg, Hôpitaux Universitaires de Strasbourg, Fédération de Médecine Translationnelle de Strasbourg, UR7290 Virulence Bactérienne Précoce, Institute of Bacteriology, Strasbourg, France

²Hôpitaux Universitaires de Strasbourg, Department of Ophthalmology, Nouvel Hôpital Civil, Strasbourg, France

³MNMS Platform, Department of Biophysics and Nuclear Medicine, Hôpitaux Universitaires de Strasbourg, Hôpital de HautePierre, Strasbourg, France

⁴Hôpitaux Universitaires de Strasbourg, Department of Dermatology, Nouvel Hôpital Civil, Strasbourg, France

Correspondence: David Gaucher, University of Strasbourg, Hôpitaux Universitaires de Strasbourg, Fédération de Médecine Translationnelle de Strasbourg, UR7290 Virulence Bactérienne Précoce, Institute of Bacteriology, 3 rue Koeberlé, F-67000 Strasbourg, France; david.gaucher@chru-strasbourg.fr.

Received: August 31, 2020

Accepted: December 4, 2020

Published: January 4, 2021

Citation: Wurtz M, Ruhland E, Liu X, et al. Panton-valentine leucocidin of *Staphylococcus aureus* induces oxidative stress and neurotransmitter imbalance in a retinal explant model. *Invest Ophthalmol Vis Sci*. 2021;62(1):4. <https://doi.org/10.1167/iovs.62.1.4>

PURPOSE. Endophthalmitis models have reported the virulent role of Panton-Valentine leucocidin (PVL) secreted by *Staphylococcus aureus* on the retina. PVL targets retinal ganglion cells (RGCs), expressing PVL membrane receptor C5aR. Interactions between PVL and retinal cells lead to glial activation, retinal inflammation, and apoptosis. In this study, we explored oxidative stress and retinal neurotransmitters in a rabbit retinal explant model incubated with PVL.

METHODS. Reactive oxygen species (ROS) production in RGCs has been assessed with fluorescent probes and immunohistochemistry. Nuclear magnetic resonance (NMR) spectroscopy quantified retinal concentrations of antioxidant molecules and neurotransmitters, and concentrations of neurotransmitters released in the culture medium. Quantifying the expression of some pro-inflammatory and anti-inflammatory factors was performed using RT-qPCR.

RESULTS. PVL induced a mitochondrial ROS production in RGCs after four hours' incubation with the toxin. Enzymatic sources of ROS, involving nicotinamide adenine dinucleotide phosphate-oxidase and xanthine oxidase, were also activated after four hours in PVL-treated retinal explants. Retinal antioxidants defenses, that is, glutathione, ascorbate and taurine, decreased after two hours' incubation with PVL. Glutamate retinal concentrations and glutamate release in the culture medium remained unaltered in PVL-treated retinas. GABA, glycine, and acetylcholine (ACh) retinal concentrations decreased after PVL treatment. Glycine release in the culture medium decreased, whereas ACh release increased after PVL treatment. Expression of proinflammatory and anti-inflammatory cytokines remained unchanged in PVL-treated explants.

CONCLUSIONS. PVL activates oxidative pathways and alters neurotransmitter retinal concentrations and release, supporting the hypothesis that PVL could induce a neurogenic inflammation in the retina.

Keywords: Panton-Valentine leucocidin, oxidative stress, antioxidant, neurotransmitter, retinal explant

Bacterial endophthalmitis is a severe ocular infection occurring in most cases after traumatism or surgery. *Staphylococcus aureus* is found in approximately 20% of cases of endophthalmitis.¹ A wide range of virulence factors synthesized by *S. aureus* has been identified. Among them, Panton-Valentine leucocidin (PVL) is of particular interest. PVL is involved in severe necrotic infections of the skin, pneumonitis, and osteomyelitis and is present in most community-acquired methicillin-resistant *S. aureus* (CA-MRSA) strains.^{2–4} The prevalence of CA-MRSA is continuously increasing and represents a major threat to address because of its resistance to antimicrobial treatments.⁵ PVL

is understood as a pore-forming toxin, composed of two subunits LukS-PV and LukF-PV, which organize in an alternate octamer.⁶ LukS-PV specifically binds to the C5a membrane receptor (C5aR) in humans and rabbits, but not in mice or rats, on account of a species polymorphism of C5aR.⁷ After injection in the vitreous of the rabbit's eye, PVL causes a significant inflammatory reaction, retinal necrosis, and the breakdown of the blood-retinal barrier (BRB).^{8,9} Glial reaction was also observed in rabbit retinal explants infected by PVL.¹⁰ Liu et al.¹¹ recently reported that PVL targets rabbit retinal ganglion cells (RGCs) expressing C5aR. RGCs are long-projection neurons that send visual

information from the retina to the brain. Rabbit retinal infection with PVL induces in vivo a glial reaction, microglial apoptosis, and an inflammatory reaction in the retina with production of interleukin (IL)-6.¹¹ The mechanisms leading to this production of inflammatory cytokines are still unclear. Indeed, IL-6 is probably secreted by infiltrated leucocytes in the retina more than by retinal glial cells. Retinal neurons are not known to produce IL-6, and in vitro experiments on rabbit retinal explants demonstrated recently that IL-6 was not overexpressed after PVL treatment.¹⁰ We hypothesized that retinal inflammation observed after RGCs infection by PVL could be mediated directly by neurons. At least two pathways could be involved: oxidative stress or neurogenic inflammatory response.

In rabbit retinas, PVL induces the production of nitrated proteins, an indirect hallmark of reactive nitrogen species (RNS) production by NO synthase.¹¹ But a direct evidence of ROS production in PVL-treated retinas has not been demonstrated yet. Oxidative stress results from an imbalance between pro-oxidant and antioxidant factors. Regulation of the retinal redox homeostasis relies on nonenzymatic antioxidants, such as ascorbate, glutathione, and vitamins A and E, that are present at high concentrations in the retina.¹² The outcome of antioxidants in PVL-treated retinas could provide further evidence of a PVL-induced oxidative stress in the retina.

PVL induces the apoptosis of amacrine and microglial cells in rabbit retinal explants.¹⁰ One hypothesis for this PVL-induced apoptosis could be glutamate excitotoxicity, that is, excessive glutamatergic stimulation secondary to massive glutamate release, leading to glial reaction and neuron cell death. In cultured rat cerebellar neurons, PVL triggers an increase in free intracellular Ca^{2+} , followed by an important glutamate release.¹³ A rise of $[\text{Ca}^{2+}]_i$ has also been measured in PVL-infected sensory neurons from dorsal root ganglia, demonstrating that PVL toxicity is not restricted to a single neuron cell type.¹³

To study the effects of PVL on retinal cells, we used a rabbit retinal explant model that we previously developed.¹⁰ Retinal explants display the advantage of maintaining the cellular microenvironment, contrary to a primary cell culture that requires tissue dissociation.

The purpose of this work was to study the effects of PVL on oxidative pathways and retinal neurotransmitters in a rabbit retinal explant model. We focused our attention on RGCs, expressing the PVL membrane receptor C5aR.¹⁰

MATERIALS AND METHODS

PVL Purification

LukS-PV and LukF-PV subunits from the strain *S. aureus* V8 (ATCC 49775) were fused to the glutathione-S-transferase (GST) gene in the plasmid pGEX6P-1 (GE-Healthcare, Chicago, IL, USA). The plasmid was transfected into the strain *Escherichia coli* BL21. After culture, induction with IPTG and lysis of *E. coli*, each protein was purified by affinity chromatography (Glutathion Sepharose 4B; Sigma-Aldrich Corp., St. Louis, MO, USA). After elution, the GST tag was removed using PreScission Protease (GE-Healthcare). A cation exchange chromatography ended the purification of LukS-PV and LukF-PV. The purity of each subunit was assessed by SDS-PAGE.¹⁴

Retinal Explant Culture and Incubation with PVL

The surgical procedure followed the guidelines of the Association for Research in Vision and Ophthalmology in an agreed animal facility D67-484-31. Rabbits (strain HY79b, Hypharm) aged 12 months and weighing 3 to 3.5 kg were anesthetized by an intramuscular injection of ketamine (20 mg/kg) and xylazine (5 mg/kg) (Bayer Healthcare, Leverkusen, Germany) followed by a lethal intravenous injection of 2 mL of pentobarbital (Vetoquinol). After enucleation, the eyes were dissected in CO_2 -independent medium (Gibco; Thermo Fisher Scientific, Waltham, MA, USA) as previously described.¹⁰ Briefly, the retina was separated from the pigment epithelium and choroid. Each retina was divided into 6 retinal explants (7×7 mm). Retinal explants were deposited on a semi-permeable membrane in a Transwell insert (Corning Inc., Corning, NY, USA), with the photoreceptor layer facing down. The insert was placed in a culture dish filled with 2 mL of culture medium (Neurobasal A medium, Thermo Fisher Scientific), supplemented with 1% (v/v) antibiotic-antimycotic solution (penicillin 20 mM and streptomycin 5 mM). PVL was diluted in culture medium (Neurobasal A medium) to a reference concentration of 1.76 μM , that had previously been used on rabbit retinal explants.¹⁰ A droplet of 10 μL (100 μg of toxin) was deposited on the surface of rabbit retinal explants. Rabbit retinal explants were incubated in the dark with the toxin for one, two, four, or eight hours, at 37°C with 5% CO_2 . An equal volume of culture medium was deposited on the surface of control explants.

Oxidative Stress Inhibitors

The respiratory chain of mitochondria and some enzymes, such as nicotinamide adenine dinucleotide phosphate (NADPH)-oxidase and xanthine oxidase, can generate free radicals.¹⁵ The 2,4-dinitrophenol (DNP) is a mitochondrial uncoupling agent that inhibits the production of free radicals in mitochondria.¹⁶ DNP was diluted to a concentration of 1 μM and 750 μM in the culture medium (Neurobasal A medium). Diphenylene iodonium (DPI) is an inhibitor of NADPH-oxidase (NOX) and was diluted to a concentration of 20 μM in the culture medium.¹⁵ The inhibitor of xanthine oxidase, allopurinol, was diluted at a concentration of 1 mM in culture medium.¹⁷ Each of these inhibitors was incubated with the rabbit retinal explants for one hour, before incubation with the toxin.

Fluorescent Probes

The production of free radicals in mitochondria was assessed with MitoSOX (Invitrogen, Carlsbad, CA, USA), a fluorescent probe that is specifically oxidized by superoxide radicals ($\text{O}_2^{\cdot-}$) in mitochondria.¹⁸ In its reduced state, MitoSOX is nonfluorescent, whereas it emits a red fluorescence when oxidized.¹⁸ MitoSOX was solubilized at 5 mM in 100% DMSO and then diluted to 5 μM in Hanks' balanced salt solution. Once the incubation with the toxin was completed, rabbit retinal explants were incubated with the solution of 5 μM MitoSOX for 10 minutes at 37°C. MitoSOX is membrane-permeant and was directly deposited on the surface of the explants. After three washes with culture medium, the explants were fixed with 4% (v/v) paraformaldehyde for one hour at 4°C.

The cytosolic production of free radicals was evaluated with dihydrorhodamine 123 (DHR), a membrane-permeant fluorescent probe that can be oxidized by superoxide radical ($O_2^{\cdot-}$), hydroxyl radical (HO^{\cdot}), hydrogen peroxide (H_2O_2) and peroxynitrite ($ONOO^-$).¹⁸ The reduced form of DHR is nonfluorescent, whereas its oxidized form emits a green fluorescence.¹⁸ DHR was solubilized at 10 mM in 100% DMSO and then diluted to 10 μ M in culture medium. After incubation with the toxin, rabbit retinal explants were incubated with the solution of 10 μ M DHR for one hour at 37°C. Retinal explants were washed three times with culture medium before fixation with 4% (v/v) paraformaldehyde for one hour at 4°C.

After incubation with either MitoSOX or DHR and after fixation, rabbit retinal explants were cryoprotected in sucrose baths overnight at 4°C. Explants were embedded in inclusion medium (Optimal Cutting Temperature, Sakura Finetek) and frozen at -80°C. Transversal retinal cryosections of 8 mm thickness were obtained with a cryomicrotome (Leica, Wetzlar, Germany) mounted on SuperFrost Plus slides (ThermoFisher Scientific, Waltham, MA, USA) and stored at -20°C.

Immunolabeling

Retinal sections were permeabilized in 0.05% (v/v) Triton X-100 for one hour. They were incubated for one hour with blockade serum, a mixture of 5% (w/v) normal goat serum (Abcam, Cambridge, MA, USA) and 1% (w/v) BSA. Retinal sections were incubated for two hours at room temperature in a humid chamber with an anti-RNA binding protein with multiple splicing (RBPMS) primary antibody directed against RGCs (Guinea Pig anti-RBPMS polyclonal antibody, 2 μ g/mL; Sigma-Aldrich). After three washes with PBS, retinal sections were incubated with fluorescent secondary antibodies in the same conditions (goat anti-IgG polyclonal Alexa Fluor 488 nm, 2 μ g/mL [Abcam] or goat anti-IgG polyclonal Alexa Fluor 594 nm, 2 μ g/mL [Abcam]). After three washes with PBS, sections were counterstained with Hoescht 33258 for 30 minutes and were mounted in 10% (v/v) Mowiol solution (Polysciences, Warrington, PA, USA).

Microscopy

Images of immunolabeled sections were obtained with an epifluorescence Olympus BX60 microscope (magnification $\times 200$) connected to a Hamamatsu C11440 digital camera (Hamamatsu Photonics, Hamamatsu City, Japan). The dimensions of the microscopic field captured by the camera were 300 \times 300 μ m. RGCs cells were identified on the sections by immunolabeling with an anti-RBPMS antibody. Colocalization of the fluorescent probe (MitoSOX or DHR) with anti-RBPMS antibodies was analyzed on the sections. MitoSOX-positive and DHR-positive RGCs were counted on three

different explants (for each explant, RGCs were counted on five retinal sections) and were expressed as a percentage of all RGCs. Fluorescence intensity of the fluorescent probes (MitoSOX and DHR) was recorded within RGCs with a constant exposure time of 600 msec. The mean fluorescence intensity within RGCs was quantified in arbitrary units, using 16-bit images analyzed with ImageJ. For each study field, the fluorescent background was measured in three microscopic areas without cells and was subtracted to the mean fluorescence measured in RGCs. Mean fluorescence intensity was measured in RGCs of three different explants (five microscopic fields were analyzed for each explant).

Nuclear Magnetic Resonance Spectroscopy

Quantification of antioxidant molecules and neurotransmitters in rabbit retinal explants and in the culture medium was measured using nuclear magnetic resonance (NMR) spectroscopy as previously described.¹⁹ Briefly, each retinal explant was placed in a single-use 25 μ L insert. 10 μ L of deuterium oxide (D_2O) were added in the insert. After centrifugation at 5000g for five minutes, deuterium oxide was added again to fill the insert. For culture medium, 15 μ L of medium was poured in the 25 μ L insert, and 10 μ L of deuterium oxide was added. NMR experiments were conducted on a Bruker Avance III 500 MHz NMR spectrometer (Bruker BioSpin, Billerica, MA, USA) at 4°C. The spectrometer was equipped with a triple-resonance (1H , ^{13}C , ^{31}P) HRMAS (High Resolution Magic Angle Spinning) probe. Metabolites were identified with different sequences: total correlation spectroscopy, heteronuclear single quantum coherence, and Carr-Purcell-Meiboom-Gill.¹⁹ Spectra obtained were analyzed with the quantification software Chenomx (Edmonton, Canada), and the amount of each metabolite was expressed in nanomoles per milligram of tissue. Mean retinal concentrations of each metabolite have been established after analyzing six rabbit retinal explants.

Real-Time-qPCR

In total 500 μ L TRIzol reagent (Sigma-Aldrich) was poured into tubes containing the frozen rabbit retinal explants. Retinal tissue was homogenized in the tube and incubated for five minutes at room temperature. Total RNA was extracted with TRIzol reagent according to the manufacturer's instructions. Total RNA concentration was quantified using spectrophotometry (NanoDrop; ThermoFisher Scientific). Total RNA was treated with DNase I (Sigma-Aldrich) at room temperature for 15 minutes according to manufacturer's instructions. Reverse transcription (RT) was performed using Superscript II Reverse Transcriptase (Invitrogen). The RT mixture contained 1 μ g total RNA, 1 μ L random primers (500 μ g/mL), 1 μ L dNTP mix (10 mM), and 5 μ L DEPC-

TABLE. Sequences of Forward and Reverse Primers Used in the Study

Gene Name	Forward Primer	Reverse Primer
β -actin	5'-CGCATGCAGAAGGAGATCAC-3'	5'-CGACTCGTCATACTCCTGCT-3'
COX 2	5'-GGGACATGGGGTGGAAGTAA-3'	5'-TGTGAGGCGGGTAGATCATC-3'
IL 4	5'-GCAGTTCTACCTCCACCACA-3'	5'-ATTCTCTTGCATGGCGGTC-3'
IL 10	5'-TTGTAAACCGAGTCCCTGCT-3'	5'-CCACTGCCTTGCTCTTGTTT-3'
IL 12	5'-CACGGTGAAGGCCTGTTAC-3'	5'-AAGCTTTGCATTCATGGCCA-3'
TGF- β	5'-CTTCCCTCCGAAACTGTCT-3'	5'-CCACTCTGGCTTTTGGGTTC-3'

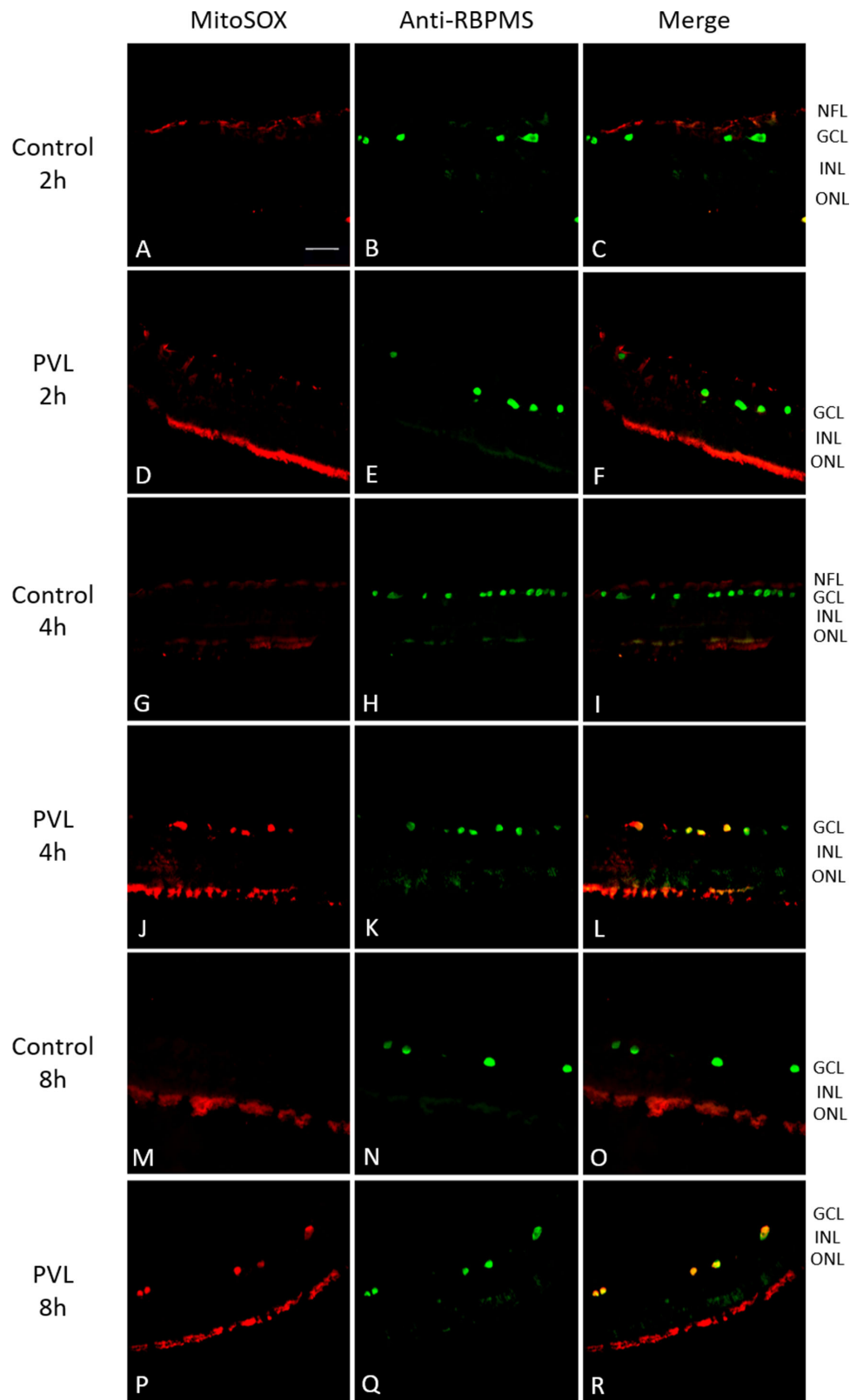


FIGURE 1. A double labeling with MitoSOX and anti-RBPMS antibody was used to assess mitochondrial ROS production in RGCs of rabbit retinal explants. Two hours after PVL treatment, the proportion of MitoSOX-positive RGCs did not differ between PVL-treated explants and controls (A–F and S). MitoSOX-positive RGCs significantly increased in rabbit retinal explants four and eight hours after PVL treatment compared to controls (G–R and S). Results are expressed as mean \pm SEM; * $P < 0.05$; ** $P < 0.01$; *** $P < 0.001$; scale bar: 50 μ m. GCL, ganglion cell layer; INL, inner nuclear layer; NFL, nerve fiber layer; ONL, outer nuclear layer; RBPMS, RNA binding protein with multiple splicing.

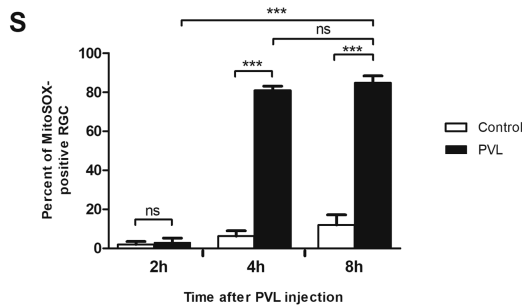


FIGURE 1. Continued

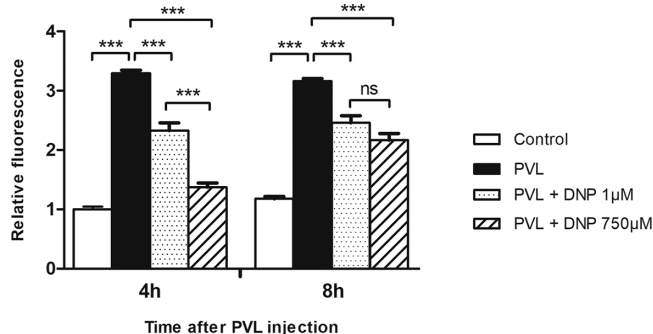


FIGURE 2. Mitochondrial ROS quantification in RGCs of rabbit retinal explants four and eight hours after PVL treatment. Mitochondrial ROS quantification was assessed by measuring the MitoSOX fluorescence in RGCs on retinal cross-sections. Fluorescence intensity values from control explants after four hours of incubation were used to normalize the results. In PVL-treated explants, ROS production increased significantly 4h and 8h after PVL treatment. Pharmacologic inhibition with 1 μ M DNP or 750 μ M DNP, a mitochondrial uncoupling agent, significantly reduced ROS production in RGCs four and eight hours after PVL treatment. Results are expressed as mean \pm SEM; * $P < 0.05$; ** $P < 0.01$; *** $P < 0.001$.

treated water. After heating at 65°C for five minutes, the mixture was chilled on ice for five minutes. Then, 4 μ L of 5X First Strand Buffer, 2 μ L of DTT (0.1 M), 1 μ L of RT (200 units), and 1 μ L of DEPC-treated water were added to the mixture. The RT mixture was incubated in a thermocycler at 42°C for 50 minutes and at 70°C for 15 minutes. The quantitative PCR was performed with the LightCycler 480 SYBR Green I Master kit (Roche, Mannheim, Germany). The PCR mix was prepared in a 96-well plate, and each well contained 5 μ L of cDNA, 10 μ L of Master Mix, 2 μ L of forward and reverse primers (10 μ M), and 3 μ L of PCR-grade water. The plate was placed in a Real-Time PCR platform (LightCycler 480; Roche). The amplification program began with an initial denaturation step (95°C for 10 minutes), followed by 45 cycles of amplification (denaturation at 95°C for 15 seconds, annealing at 60°C for 20 seconds, and extension at 72°C for 15 seconds), and a melting curve analysis (60°C to 95°C, increment +0.1°C/sec). The specificity of PCR amplification products was checked by detecting a single melting curve peak. The absence of amplification products in wells without RT ascertained no significant DNA contamination occurred. The primers were designed with Primer3 software (version 4.1.0, <http://primer3.ut.ee/>) and had a melting temperature (T_m) around 60°C. The sequences of forward and reverse primers are described in the Table.

The β -actin was used as a housekeeping gene, and target genes were normalized using this reference gene. The $\Delta\Delta C_t$

method was used to estimate the relative expression of the genes between control and PVL-treated explants. Expression fold changes were calculated using the $2^{-\Delta\Delta C_t}$ method. The tests were made in triplicate.

Statistical Analysis

Unpaired Student's *t*-tests were used to compare data between PVL-treated explants and controls. Multiple comparison tests were performed using one-way ANOVA followed by Tukey's *post hoc* test (GraphPad Prism 5 software; GraphPad, San Diego, CA, USA). Statistical significance was defined as $P < 0.05$. Results are expressed as mean \pm SEM.

RESULTS

PVL Induces Mitochondrial ROS Production in RGCs

In the rabbit, PVL targets RGCs both in vivo and in the retinal explant model.^{10,11} Double labeling with MitoSOX and anti-RBPMS antibody was used to study the mitochondrial ROS production in RGCs of rabbit retinal explants. The proportion of MitoSOX-positive RGCs remained unchanged after two hours' PVL incubation compared to controls ($3.1\% \pm 2.2\%$ vs. $2.0\% \pm 1.5\%$; $P > 0.05$, Figs. 1A–1F, 1S). However, after four hours' PVL treatment, MitoSOX-positive RGCs significantly increased, to reach respectively $80.9\% \pm 2.2\%$ of total RGCs compared with $6.3\% \pm 2.7\%$ in controls ($P < 0.001$, Figs. 1G–1L, 1S), and $84.8\% \pm 3.6\%$ after eight hours versus $12.1\% \pm 5.1\%$ in controls ($P < 0.001$, Figs. 1M–1R, 1S). Relative quantification of ROS production in RGCs assessed that the amount of mitochondrial ROS increased in PVL-treated RGCs. ROS production in PVL-treated RGCs was 3.3-fold higher than the one of control RGCs after four hours ($P < 0.001$, Fig. 2) and 2.7-fold higher after eight hours ($P < 0.001$, Fig. 2). To confirm the mitochondrial origin of the ROS detected with MitoSOX, we used DNP, a mitochondrial uncoupling agent that annihilates the mitochondrial proton gradient. Both 1 μ M DNP and 750 μ M DNP inhibited ROS production in PVL-treated RGCs, respectively, by 29.3% ($P < 0.001$, Fig. 2) and 58.2% ($P < 0.001$, Fig. 2) after four hours, and by 22.2% ($P < 0.001$, Fig. 2) and 31.5% ($P < 0.001$, Fig. 2) after eight hours. These results suggest that PVL induces a mitochondrial ROS production in RGCs of rabbit retinal explants within the few hours after PVL treatment.

PVL Induces Enzymatic ROS Production in RGCs

Double labeling with DHR and anti-RBPMS antibody was used to evaluate the cytosolic ROS production in RGCs of rabbit retinal explants. The proportion of DHR-positive RGCs remained unchanged after two hours' PVL incubation ($5.4\% \pm 3.4\%$ vs. $1.5\% \pm 1.0\%$; $P > 0.05$, Figs. 3A–3F, 3S). DHR-positive RGCs significantly increased after four and eight hours' PVL incubation to reach, respectively, $77.0\% \pm 4.2\%$ of the total RGCs versus $7.9\% \pm 4.6\%$ in controls after four hours ($P < 0.001$, Figs. 3G–3L, 3S) and $92.8\% \pm 2.5\%$ versus $11.6\% \pm 2.8\%$ after eight hours ($P < 0.001$, Figs. 3M–3R, 3S). Relative ROS quantification in RGCs showed that the amount of cytosolic ROS increased in PVL-treated RGCs. ROS production in PVL-treated RGCs was 2.2-fold higher than the one in controls after four hours ($P < 0.001$, Fig. 4) and 2.3-fold higher after eight hours ($P < 0.001$, Fig. 4). To assess the

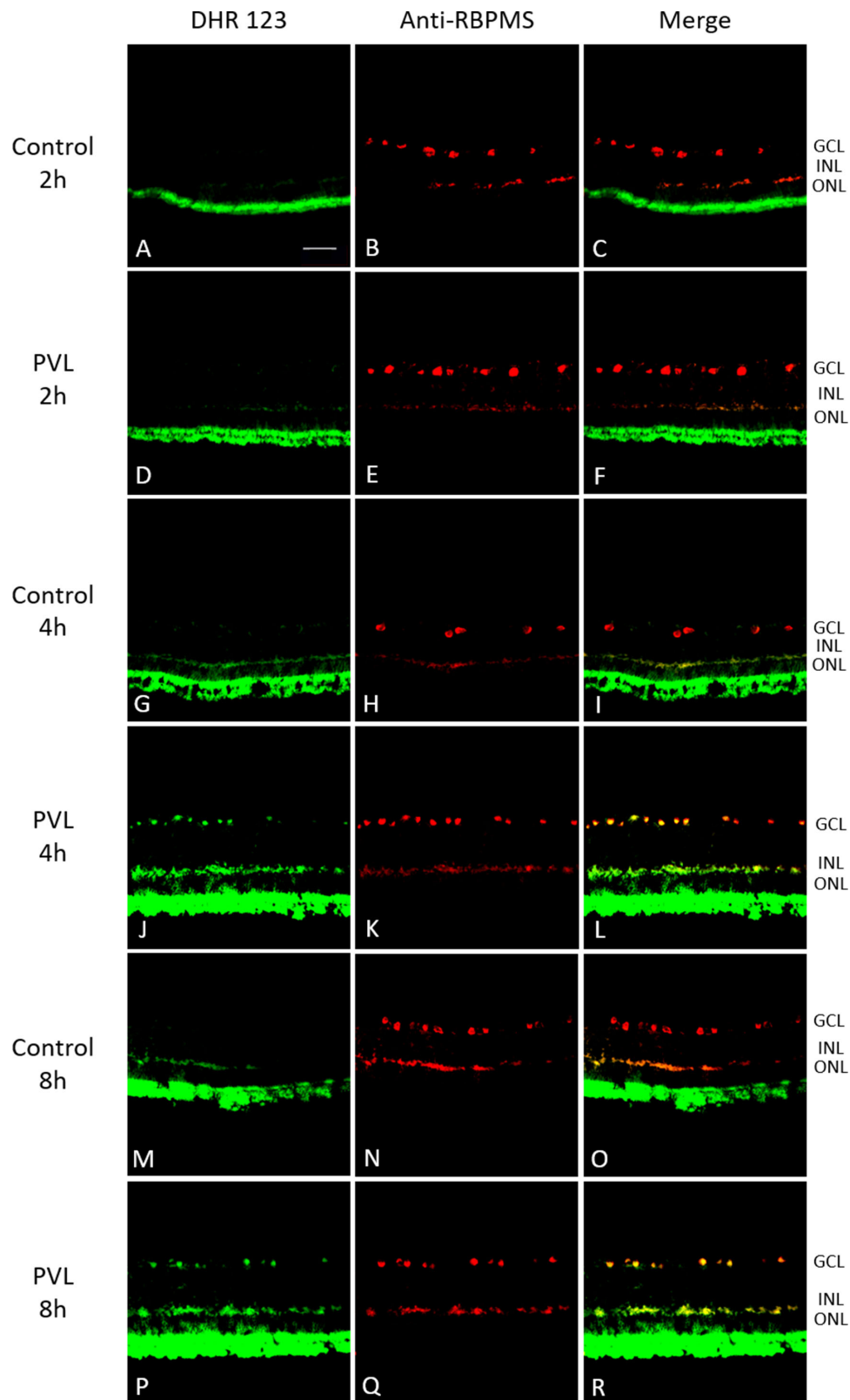


FIGURE 3. A double labeling with dihydrorhodamine 123 and anti-RBPMS antibody was used to assess cytosolic ROS production in RGCs of rabbit retinal explants. Two hours after PVL treatment, the proportion of DHR-positive RGCs did not differ between PVL-treated explants and controls (**A–F** and **S**). DHR-positive RGCs significantly increased four and eight hours after PVL treatment compared to controls (**G–R** and **S**). Results are expressed as mean \pm SEM; * $P < 0.05$; ** $P < 0.01$; *** $P < 0.001$; scale bar: 50 μ m. GCL, ganglion cell layer; INL, inner nuclear layer; NFL, nerve fiber layer; ONL, outer nuclear layer; RBPMS, RNA binding protein with multiple splicing.

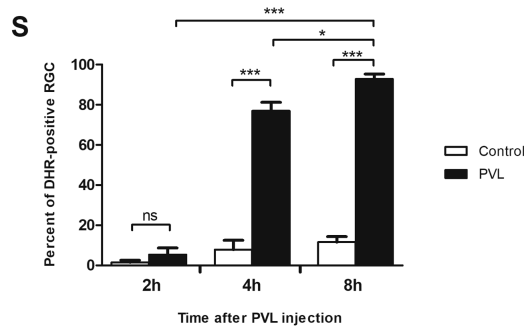


FIGURE 3. Continued

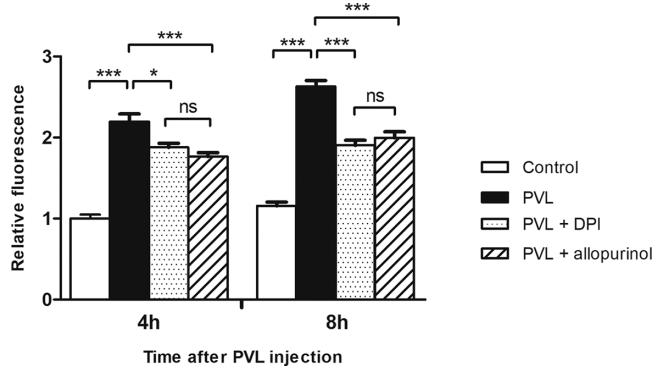


FIGURE 4. Cytosolic ROS quantification in RGCs of rabbit retinal explants four and eight hours after PVL treatment. Cytosolic ROS quantification was assessed by measuring DHR fluorescence in RGCs on retinal cross-sections. Fluorescence intensity values from control explants after four hours of incubation were used to normalize the results. In PVL-treated explants, ROS production increased significantly four and eight hours after PVL treatment. Pharmacologic inhibition with DPI or allopurinol, respectively inhibiting NADPH-oxidase and xanthine oxidase, significantly reduced ROS production in RGCs four and eight hours after PVL treatment. Results are expressed as mean \pm SEM; * $P < 0.05$; ** $P < 0.01$; *** $P < 0.001$.

origin of these ROS, we used DPI and allopurinol, respectively, to inhibit NADPH-oxidase and xanthine oxidase. DPI reduced ROS synthesis in PVL-treated RGCs by 14.5% after four hours ($P < 0.05$, Fig. 4), and by 27.6% after eight hours ($P < 0.001$, Fig. 4). Allopurinol reduced ROS synthesis in PVL-treated RGCs by 19.6% after four hours ($P < 0.001$, Fig. 4), and by 24.1% after eight hours ($P < 0.001$, Fig. 4). These results suggest that NADPH-oxidase and xanthine oxidase are both enzymes involved in ROS production in PVL-treated rabbit retinal explants. Taken together, these results reveal that PVL induces both mitochondrial and enzymatic oxidative pathways in RGCs of rabbit retinal explants.

PVL Induces a Drop of Antioxidant Molecules in Retinal Explants

The redox state of a cell relies on a balance between pro-oxidant and antioxidant molecules. We analyzed retinal concentrations of glutathione, taurine and ascorbate, three nonenzymatic molecules with antioxidant properties, in PVL-treated and in control rabbit retinal explants.^{12,20} After one and two hours of PVL incubation, retinal concentrations of glutathione, taurine, and ascorbate were significantly reduced compared to control explants. Glutathione

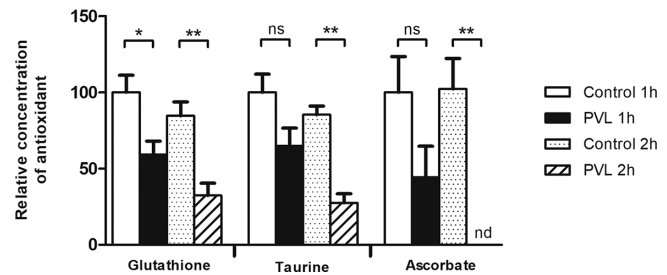


FIGURE 5. Relative concentrations of antioxidant molecules in PVL-treated rabbit retinal explants after one and two hours' incubation. Concentration values from control explants after one hour of incubation were used to normalize the results. Glutathione concentration decreased significantly one and two hours after PVL treatment. Taurine and ascorbate concentrations significantly decreased two hours after PVL treatment. Ascorbate was undetectable after two hours in PVL-treated explants. Results are expressed as mean \pm SEM; * $P < 0.05$; ** $P < 0.01$; *** $P < 0.001$; $n = 6$ explants. nd, not detected.

retinal concentration in PVL-treated explants decreased by 40.8% ($P < 0.05$, Fig. 5) after one hour, and by 61.7% after two hours ($P < 0.01$, Fig. 5) compared to controls. Taurine concentration in PVL-treated explants did not differ significantly from controls after one hour but significantly decreased by 67.7% after two hours ($P < 0.01$, Fig. 5). Ascorbate retinal concentration did not differ significantly between PVL-treated explants and controls after one hour, but decreased significantly by nearly 100% after two hours ($P < 0.01$, Fig. 5) compared to controls. Indeed, after two hours' PVL incubation, ascorbate was so reduced that it became undetectable. The drop of these antioxidant defenses seems to be an early event after PVL treatment, because all the three antioxidants decreased within the two hours after PVL treatment. Thus mitochondrial and enzymatic ROS productions are associated with a drop of antioxidant molecules, suggesting that PVL induces a shift of the redox homeostasis toward a pro-oxidative state.

PVL Alters Retinal Neurotransmitter Concentrations and Neurotransmitter Release

Excessive glutamate release can induce excitotoxicity and neuronal cell death. It has been formerly demonstrated that PVL can trigger glutamate release in a primary culture of neurons.¹³ Hence, we tested whether PVL can elicit glutamate release in our rabbit retinal explant model. In PVL-treated explants, glutamate concentration in retinal explants and glutamate release in the culture medium did not change significantly compared to control explants ($P > 0.05$, Figs. 6A, 6B). However, the concentration of the other neurotransmitters was altered in PVL-treated explants. The concentration of glycine was reduced in PVL-treated retinal explants by 43.5% after one hour ($P < 0.05$, Fig. 6A) and by 68.0% after two hours ($P < 0.001$, Fig. 6A) compared to controls. The release of glycine in the culture medium decreased by 30.2% in PVL-treated explants after two hours ($P < 0.05$, Fig. 6B). The retinal concentration of acetylcholine decreased in PVL-treated explants by 33.2% after one hour ($P < 0.05$, Fig. 6A) and by 57.3% after two hours ($P < 0.001$, Fig. 6A), whereas its concentration increased in the culture medium by 57.3% after one hour ($P < 0.05$, Fig. 6B) and by 68.7% after two hours ($P < 0.01$, Fig. 6B), suggesting that PVL

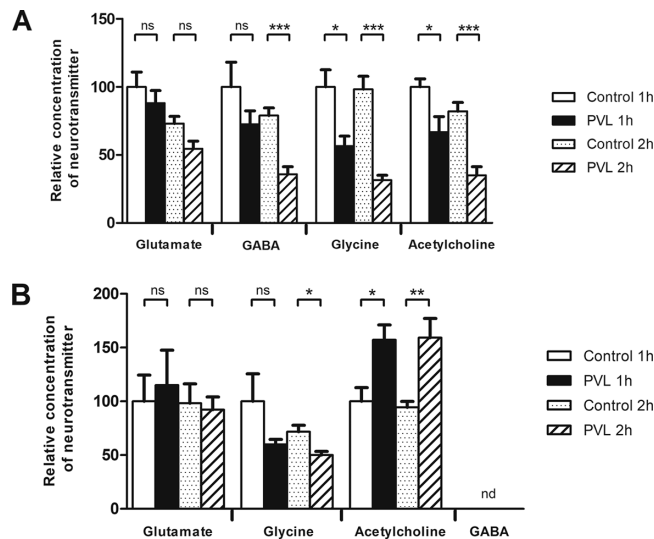


FIGURE 6. Relative concentrations of neurotransmitters in rabbit retinal explants (A), and in the culture medium of rabbit retinal explants (B), after one and two hours' incubation with PVL. Concentration values from control explants after one hour of incubation were used to normalize the results. Glutamate retinal concentrations and glutamate release in the culture medium remained unchanged after one and two hours in PVL-treated explants, compared to controls (A–B). GABA retinal concentrations decreased significantly after 2h incubation with PVL (A). GABA was not detected in the culture medium of PVL-treated and control explants (B). Glycine retinal concentrations decreased after one and two hours' incubation with PVL (A) and glycine release in the culture medium decreased after two hours (B). Acetylcholine retinal concentrations decreased after one and two hours (A) and acetylcholine release in the culture medium increased after one and two hours (B). Results are expressed as mean \pm SEM; * $P < 0.05$; ** $P < 0.01$; *** $P < 0.001$; $n = 6$ explants. nd, not detected.

induced a release of acetylcholine. GABA retinal concentration decreased in PVL-treated explants by 54.6% after two hours ($P < 0.001$, Fig. 6A). GABA was not detected in the culture medium of control and PVL-treated retinas (Fig. 6B). Taken together, these results suggest that PVL deeply disturbs the distribution of retinal neurotransmitters in rabbit retinal explants.

Expression of Proinflammatory and Anti-Inflammatory Factors in PVL-Treated Explants

We formerly demonstrated that PVL did not induce the expression of some of the most common inflammatory cytokines (IL-6, IL-8, TNF- α , VEGF) in rabbit retinal explants.¹¹ We further explored the expression profile of proinflammatory and anti-inflammatory cytokines in rabbit retinal explants after eight hours of incubation with PVL using RT-qPCR. The mRNA expression of proinflammatory cytokines (IL-4 and IL-12) was not significantly different in PVL-treated explants and in control explants ($P > 0.05$, Fig. 7). In addition, mRNA expression of anti-inflammatory cytokines IL-10 and transforming growth factor- β (TGF- β) did not differ significantly between PVL-treated explants and controls ($P > 0.05$, Fig. 7). We finally analyzed the expression of cyclooxygenase-2 (COX-2), the inducible isoform of cyclooxygenase, that synthesizes proinflammatory prostaglandins.²¹ COX-2 mRNA expression did

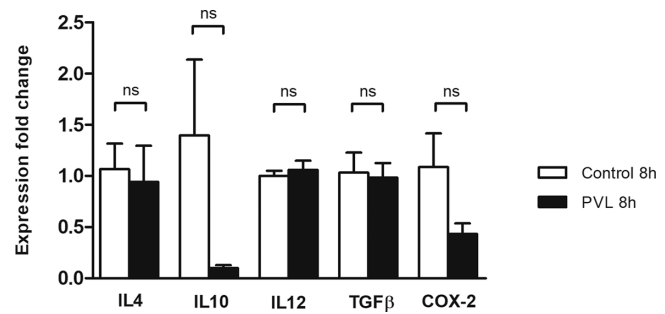


FIGURE 7. Expression of proinflammatory cytokines (IL-4 and IL-12), anti-inflammatory cytokines (IL-10 and TGF- β) and COX-2 enzyme after eight hours' incubation in PVL-treated and control rabbit retinal explants. β -actin was used as a housekeeping gene, and target genes were normalized using this reference gene. Relative gene expression of cytokines and COX-2 enzyme remained unchanged after eight hours in both PVL-treated and control explants. Results are expressed as mean \pm SEM; * $P < 0.05$; ** $P < 0.01$; *** $P < 0.001$; $n = 3$ explants.

not change significantly in PVL-treated explants compared to controls ($P > 0.05$, Fig. 7). Consequently, IL-4, IL-10, IL-12, TGF- β , and COX-2 do not seem to trigger the inflammatory response observed in rabbit retinal explants after PVL treatment.

DISCUSSION

In the rabbit, it has been recently reported that PVL targets retinal ganglion cells, which express the membrane receptor C5aR *in vivo* and in the retinal explant model.^{10,11} The present results demonstrate that PVL also unbalances the redox state in rabbit retinal explants and particularly in RGCs. PVL activates mitochondrial and enzymatic oxidative pathways, resulting in ROS production. On the other hand, PVL may induce a decrease of antioxidant defenses because glutathione, taurine and ascorbate are reduced after PVL treatment, at least in the rabbit retinal explant model.

These results are in accordance with a previous observation that PVL induced oxidative stress in the retina. Indeed, Liu et al.¹¹ reported that PVL increased the production of RNS in rabbit retinal explants only four hours after PVL treatment.

The present results showed that DNP, a mitochondrial uncoupling agent, inhibited ROS production, suggesting that the mitochondrial respiratory chain was a source of ROS in PVL-treated RGCs. In our study, pharmacologic inhibition of NADPH-oxidase and xanthine oxidase activities demonstrated that enzymatic oxidative pathways are also involved in PVL-induced RGCs ROS production. Initially, PVL-induced oxidative stress has been assessed in human polymorphonuclear neutrophils (hPMNs) that express PVL membrane receptor C5aR.²² In hPMNs, PVL activates NADPH-oxidase and myeloperoxidase, leading to a release of superoxide radical ($O_2^{\cdot-}$).²³ In our rabbit retinal explants, inhibition of NADPH-oxidase and xanthine oxidase only partially decreased PVL-induced ROS production, suggesting that other enzymatic sources of ROS could be activated by PVL, such as myeloperoxidase or lipoxygenase, two oxidative enzymes expressed in the retina.^{24,25}

Oxidative stress is the result of an imbalance between ROS production and antioxidant defenses. The present study

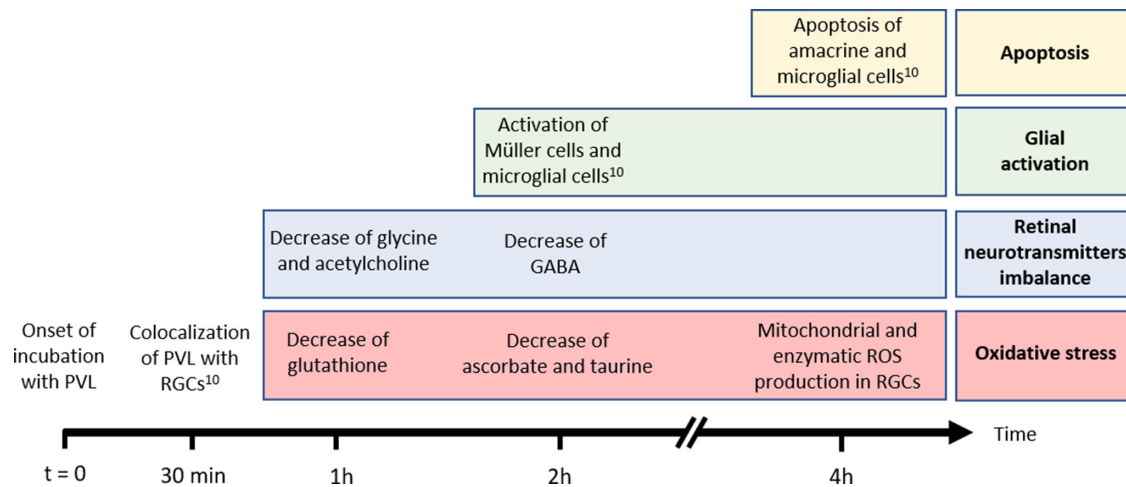


FIGURE 8. Timeline describing the chronology of inflammatory events in rabbit retinal explants incubated with PVL. PVL targets RGCs of rabbit retinal explants only 30 min after the onset of the incubation, as described by Liu et al.¹⁰. In the present study, we demonstrated that PVL unbalances the redox state in retinal explants. Incubation with PVL induces an early decrease of antioxidant defenses and activates mitochondrial and enzymatic oxidative pathways, resulting in ROS production. PVL alters the homeostasis of retinal neurotransmitters with a decrease of glycine, GABA and acetylcholine retinal concentrations. Liu et al.¹⁰ previously reported glial activation and cell apoptosis in PVL-treated explants. But oxidative stress and neurotransmitters imbalance seem to be earlier events than glial activation and cell apoptosis. This chronology suggests that oxidative stress and neurotransmitters imbalance could be involved in the early initiation of retinal inflammation, supporting the hypothesis of a neurogenic inflammation in PVL-treated retinal explants.

demonstrated that PVL treatment decreases retinal concentrations of glutathione, ascorbate and taurine, three nonenzymatic molecules involved in the redox homeostasis.¹² The drop of these antioxidants could reveal the switch from their reduced form to their oxidized form. Kamegawa et al.²⁶ similarly reported a fall of the reduced form of several antioxidants, such as glutathione, ascorbate, and vitamin E in rabbit retinas a few hours after a pro-oxidative molecule (lipid hydroperoxide) was injected intravitreally. The present study showed that the antioxidant decrease is an early event after PVL treatment, because glutathione, taurine, and ascorbate dropped strongly only two hours after incubation with the toxin. This observation might explain why oxidative stress fluorescent probes (MitoSOX and DHR) did not reveal any ROS production before four hours after PVL treatment: this chronology suggests that in the early phase of PVL infection, antioxidant molecules could regulate the redox homeostasis in the retina. In a second phase, antioxidant mechanisms could be saturated, or their regeneration could be impaired, leading to a switch towards a pro-oxidative state in the retina (Fig. 8). Liu et al.¹¹ also detected an increase in oxidative stress (i.e., reactive nitrogen species) four hours after PVL treatment. Of note, PVL is detected on its target RGCs in rabbit retinal explants after 30 minutes' exposure.¹¹ Our results suggest that oxidative stress could be an early event after PVL infection and could thus induce damage to proteins, lipids, carbohydrates and nucleic acids soon after the onset of an endophthalmitis. Intravitreal antibiotics used to treat endophthalmitis are effective to eliminate the pathogen but have no effect on oxidative stress or secreted toxins.¹ Thus targeting pro-oxidative mechanisms or supplying antioxidant defenses could be promising ways to explore, to limit retinal damage caused by PVL in endophthalmitis.

Apoptosis of amacrine and microglial cells has been reported in PVL-treated rabbit retinal explants.¹⁰ Apoptosis could result from glutamate excitotoxicity. Jover et al.¹³ reported that PVL can induce an important glutamate

release in cultured neurons. Hence, we tested whether PVL could elicit glutamate release in our retinal explant model. Glutamate retinal concentrations and glutamate release in the culture medium remained unchanged in PVL-treated explants, which suggests that glutamate excitotoxicity is not responsible for the cell apoptosis previously reported. Our results showed that acetylcholine concentration was reduced in PVL-treated retinal explants, whereas it was increased in their culture medium, suggesting that acetylcholine is released in the retina after PVL treatment. Acetylcholine activation of muscarinic receptors M1 and M3 was reported to stimulate the expression of NO synthase in rat retinal neurons.²⁷ NO synthase is an oxidative enzyme involved in RNS synthesis.^{27,28} Liu et al.¹¹ reported that PVL can induce RNS production in PVL-treated explants. Hence, release of acetylcholine could be a potential way of NO synthase activation and oxidative species production after PVL infection. It is interesting to note that acetylcholine stimulation of $\alpha 7$ -nicotinic receptor could also display a neuroprotective effect as already demonstrated in cases of glutamate excitotoxicity.²⁹

If neurotoxic neurotransmitters may be released in retinas after PVL treatment, we also observed in retinal explants, a concentration drop of some neuroprotective neurotransmitters such as GABA and glycine. GABA is a hyperpolarizing neurotransmitter, and its retinal concentrations were reduced in PVL-treated explants. GABA_A receptor is considered to display neuroprotective effects.³⁰ Indeed, GABA-induced membrane hyperpolarization can for instance prevent Ca^{2+} influx, which leads to apoptosis.³¹ The drop of GABA retinal concentrations could impair this protective mechanism in PVL-treated explants. Glycine is part of the antioxidant defenses of the cells, because glycine is a component of glutathione (γ -L-glutamyl-cysteinyl-glycine).³² Our rabbit retinal explant model showed that glycine concentrations were reduced in PVL-treated explants and in the culture medium of PVL-treated explants. We can hypothesize that glycine is consumed under oxidative conditions to

generate glutathione in PVL-treated explants, thus explaining the decrease of glycine concentrations.

Although culture medium cannot be considered as a physiological fluid compartment, we used culture medium to indirectly assess the effect of PVL treatment on neurotransmitters in retinal cultures. Neurotransmitters may have diffused from the edge of retinal explants to the culture medium. We were able to detect glutamate, glycine and acetylcholine in the culture medium, but GABA was not detectable in the culture medium of PVL-treated and control explants. We could assume that GABA is less diffusible in the retina tissue. Indeed, it was reported in the brain that GABA uptake by glial cells plays a crucial role to prevent GABA diffusion away from synapses to extrasynaptic areas.³³ Another explanation could be that GABA concentration in the culture medium was too low to be detected with our NMR spectrometry method. Indeed, for the three other neurotransmitters (glutamate, glycine, acetylcholine), neurotransmitter concentrations measured in the culture medium were approximately 100-fold inferior to their retinal concentrations. GABA may certainly have diffused in the culture medium, but its concentration may have stayed below the NMR detection limit.

In the retina, proinflammatory and anti-inflammatory cytokines are secreted by retinal glial cells, in case of tissue injury or infection.^{34,35} Cytokines regulate the immune system and attract leukocytes to the harmed tissue.³⁴ In PVL-treated retinal explants, expression of the most common pro-inflammatory cytokines (IL-6, IL-8, TNF- α , VEGF) was not upregulated as previously reported by Liu et al.¹¹ Some cytokines, such as IL-10 and TGF- β , display anti-inflammatory features. Their role is to regulate the intensity of the inflammatory response.³⁶ In our study, we confirmed that the expression profile of proinflammatory and anti-inflammatory cytokines (IL-4, IL-10, IL-12, TGF- β) in PVL-treated retinal explants remained unchanged compared to control retinas. These results suggest that cytokine-mediated inflammatory pathways do not seem to be involved in the early inflammatory response following PVL infection. But oxidative stress and neurotransmitters imbalance could account for the early initiation of a neuron-mediated inflammation in PVL-treated retinas (Fig. 8). Future studies should focus on the intracellular machinery leading to oxidative stress and neurotransmitter alterations, particularly intracellular Ca²⁺ imaging, to provide further support to the hypothesis of a neurogenic inflammation in PVL retinal infection.

Acknowledgments

The authors thank Daniel Keller for toxin preparation and Viola Mazzoleni for efficient advises.

Supported by recurrent funds of UR7290, the Hôpitaux Universitaires de Strasbourg (MW), and a Chinese Doctoral International fellowship (XL).

Disclosure: **M. Wurtz**, None; **E. Ruhland**, None; **X.L. Liu**, None; **I.-J. Namer**, None; **V. Mazzoleni**, None; **D. Lipsker**, None; **D. Keller**, None; **G. Prévost**, None; **D. Gaucher**, None

References

1. Callegan MC, Engelbert M, Parke DW, Jett BD, Gilmore MS. Bacterial endophthalmitis: epidemiology, therapeutics, and bacterium-host interactions. *Clin Microbiol Rev*. 2002;15(1):111–124.

2. Vandenesch F, Naimi T, Enright MC, et al. Community-acquired methicillin-resistant *Staphylococcus aureus* carrying Panton-Valentine leukocidin genes: worldwide emergence. *Emerg Infect Dis*. 2003;9(8):978–984.
3. Couppie P, Cribier B, Prévost G. Leukocidin from *Staphylococcus aureus* and cutaneous infections: an epidemiologic study. *Arch Dermatol*. 1994;130(9):1208–1209.
4. Sina H, Ahoyo TA, Moussaoui W, et al. Variability of antibiotic susceptibility and toxin production of *Staphylococcus aureus* strains isolated from skin, soft tissue, and bone related infections. *BMC Microbiol*. 2013;13:188.
5. Diep BA, Gill SR, Chang RF, et al. Complete genome sequence of USA300, an epidemic clone of community-acquired methicillin-resistant *Staphylococcus aureus*. *Lancet Lond Engl*. 2006;367(9512):731–739.
6. Spaan AN, van Strijp JAG, Torres VJ. Leukocidins: Staphylococcal bi-component pore-forming toxins find their receptors. *Nat Rev Microbiol*. 2017;15(7):435–447.
7. Spaan AN, Schiepers A, de Haas CJC, et al. Differential interaction of the staphylococcal toxins Panton-Valentine leukocidin and γ -hemolysin CB with human C5a receptors. *J Immunol Baltim Md 1950*. 2015;195(3):1034–1043.
8. Siqueira JA, Speeg-Schatz CIS, Freitas F, Sahel J, Monteil H, Prévost G. Channel-forming leucotoxins from *Staphylococcus aureus* cause severe inflammatory reactions in a rabbit eye model. *J Med Microbiol*. 1997;46:486–494.
9. Laventie B-J, Rademaker HJ, Saleh M, et al. Heavy chain-only antibodies and tetravalent bispecific antibody neutralizing *Staphylococcus aureus* leukotoxins. *Proc Natl Acad Sci USA*. 2011;108(39):16404–16409.
10. Liu X, Roux MJ, Picaud S, et al. Panton-Valentine leukocidin proves direct neuronal targeting and its early neuronal and glial impacts a rabbit retinal explant model. *Toxins*. 2018;10(11):455.
11. Liu X, Heitz P, Roux M, et al. Panton-Valentine leukocidin colocalizes with retinal ganglion and amacrine cells and activates glial reactions and microglial apoptosis. *Sci Rep*. 2018;8(1):2953.
12. Cabrera MP, Chihuaif RH. Antioxidants and the integrity of ocular tissues. *Vet Med Int*. 2011;2011:905153.
13. Jover E, Tawk MY, Laventie B-J, Poulain B, Prévost G. Staphylococcal leukotoxins trigger free intracellular Ca(2+) rise in neurones, signalling through acidic stores and activation of store-operated channels. *Cell Microbiol*. 2013;15(5):742–758.
14. Joubert O, Viero G, Keller D, et al. Engineered covalent leucotoxin heterodimers form functional pores: insights into S-F interactions. *Biochem J*. 2006;396(2):381–389.
15. Groeger G, Mackey AM, Pettigrew CA, Bhatt L, Cotter TG. Stress-induced activation of Nox contributes to cell survival signaling via production of hydrogen peroxide. *J Neurochem*. 2009;109(5):1544–1554.
16. Abdel-Salam O, Youness E, Mohamed N, Shaffie N, Abouelfadl D, Sleem A. The effect of 2,4-dinitrophenol on oxidative stress and neuronal damage in rat brain induced by systemic rotenone injection. *React Oxyg Species*. 2017;3(8):135–147.
17. Usui S, Oveson BC, Lee SY, et al. NADPH oxidase plays a central role in cone cell death in retinitis pigmentosa. *J Neurochem*. 2009;110(3):1028–1037.
18. Forkink M, Smeitink JAM, Brock R, Willems PHGM, Koopman WJH. Detection and manipulation of mitochondrial reactive oxygen species in mammalian cells. *Biochim Biophys Acta BBA - Bioenerg*. 2010;1797(6):1034–1044.
19. Ruhland E, Bund C, Outilaft H, Piotto M, Namer I-J. A metabolic database for biomedical studies of biopsy specimens by high-resolution magic angle spinning nuclear MR: a qualitative and quantitative tool. *Magn Reson Med*. 2019;82(1):62–83.

20. Seidel U, Huebbe P, Rimbach G. Taurine: a regulator of cellular redox homeostasis and skeletal muscle function. *Mol Nutr Food Res*. 2019;63(16):e1800569.
21. Ju W-K, Neufeld AH. Cellular localization of cyclooxygenase-1 and cyclooxygenase-2 in the normal mouse, rat, and human retina. *J Comp Neurol*. 2002;452(4):392–399.
22. Spaan AN, Henry T, van Rooijen WJM, et al. The staphylococcal toxin Pantone-Valentine Leukocidin targets human C5a receptors. *Cell Host Microbe*. 2013;13(5):584–594.
23. Graves SF, Kobayashi SD, Braughton KR, et al. Sublytic concentrations of Staphylococcus aureus Pantone-Valentine leukocidin alter human PMN gene expression and enhance bactericidal capacity. *J Leukoc Biol*. 2012;92(2):361–374.
24. Khan AA, Alsahli MA, Rahmani AH. Myeloperoxidase as an active disease biomarker: recent biochemical and pathological perspectives. *Med Sci*. 2018;6(2).
25. Al-Shabrawey MA, El-Marakby A, Ahmad S, Megyerdi S, Maddipati K. Inhibition Of 12/15 Lipoyxygenase Reduces Oxidative Stress And Inflammatory Cytokines In Retina Of Diabetic Mouse. *Invest Ophthalmol Vis Sci*. 2011;52(14):4449–4449.
26. Kamegawa M, Nakanishi-Ueda T, Iwai S, et al. Effect of lipid-hydroperoxide-induced oxidative stress on vitamin E, ascorbate and glutathione in the rabbit retina. *Ophthalmic Res*. 2007;39(1):49–54.
27. Borda E, Berra A, Saravia M, Ganzinelli S, Sterin-Borda L. Correlations between neuronal nitric oxide synthase and muscarinic M3/M1 receptors in the rat retina. *Exp Eye Res*. 2005;80(3):391–399.
28. Fang FC. Perspectives series: host/pathogen interactions. Mechanisms of nitric oxide-related antimicrobial activity. *J Clin Invest*. 1997;99(12):2818–2825.
29. Thompson SA, Smith O, Linn DM, Linn CL. Acetylcholine neuroprotection against glutamate-induced excitotoxicity in adult pig retinal ganglion cells is partially mediated through alpha4 nAChRs. *Exp Eye Res*. 2006;83(5):1135–1145.
30. Muir JK, Lobner D, Monyer H, Choi DW. GABAA receptor activation attenuates excitotoxicity but exacerbates oxygen-glucose deprivation-induced neuronal injury in vitro. *J Cereb Blood Flow Metab Off J Int Soc Cereb Blood Flow Metab*. 1996;16(6):1211–1218.
31. Mayer ML, Westbrook GL, Guthrie PB. Voltage-dependent block by Mg²⁺ of NMDA responses in spinal cord neurones. *Nature*. 1984;309(5965):261–263.
32. Weinberg JM, Bienholz A, Venkatachalam MA. The role of glycine in regulated cell death. *Cell Mol Life Sci CMLS*. 2016;73(11-12):2285–2308.
33. Beenhakker MP, Huguenard JR. Astrocytes as Gatekeepers of GABAB Receptor Function. *J Neurosci*. 2010;30(45):15262–15276.
34. Kumar A, Pandey RK, Miller LJ, Singh PK, Kanwar M. Muller glia in retinal innate immunity: a perspective on their roles in endophthalmitis. *Crit Rev Immunol*. 2013;33(2):119–135.
35. Eastlake K, Banerjee PJ, Angbohang A, Charteris DG, Khaw PT, Limb GA. Müller glia as an important source of cytokines and inflammatory factors present in the gliotic retina during proliferative vitreoretinopathy. *Glia*. 2016;64(4):495–506.
36. Sanjabi S, Zenewicz LA, Kamanaka M, Flavell RA. Anti-inflammatory and pro-inflammatory roles of TGF-beta, IL-10, and IL-22 in immunity and autoimmunity. *Curr Opin Pharmacol*. 2009;9(4):447–453.